



1 Article

# 2 Rice Starch-Templated Synthesis of Nanostructured 3 Silica and Hematite

4 Juan Matmin <sup>1,\*</sup>

5 <sup>1</sup> Centre of Foundation Studies, Universiti Teknologi MARA (UiTM), Cawangan Selangor, Kampus Dengkil,  
6 43800 Dengkil, Selangor, Malaysia

7 \* Correspondence: juanmatmin@puncakalam.uitm.edu.my; Tel.: +60-389-245-449

8 Academic Editor: name

9 Received: date; Accepted: date; Published: date

10 **Abstract:** Synthesis of nanostructured materials is not straightforward which involve the  
11 complicated use of surfactant templates. Currently, only non-renewable resources that are  
12 hazardous and toxic are used to produce the surfactant templates in the industries. This study  
13 presents an environmentally friendly and efficient route for the synthesis of nanostructured of both  
14 silica and hematite using rice starch as a promising biomaterials template. The rice  
15 starch-templated synthesis yield both hematite and silica with nano-sized and high surface area. In  
16 particular, the nanostructured silica showed a pseudo-spherical morphology with nano-sized from  
17 13 to 22 nm, amorphous structure and surface area of 538.74 m<sup>2</sup>/g. On the other hand, the  
18 nanostructured hematite showed and spherical-shaped morphology with nano-sized from 24 to 48  
19 nm, and surface area of 20.04 m<sup>2</sup>/g. More importantly, the used of rice starch-template for a greener  
20 approach in the synthesis of nanomaterials have been successfully outlined.

21 **Keywords:** nanostructured materials; rice starch; template-assisted synthesis; nanoparticles  
22 hematite; porous silica; surfactant-free; additive-free; biomaterials template.  
23

## 24 1. Introduction

25 Nanostructured materials are one of the very special structures that have led to the  
26 enhancement of properties that are not available for any other materials. A variety of synthesis  
27 methods such as sol-gel process [1], sonochemical route [2], surface polymerization processes [3],  
28 colloidal templating methods and template assisted approaches have been used for the fabrication of  
29 materials with nanostructured properties [4]. Among the various synthesis methods,  
30 template-assisted approaches are considered as very efficient, most effective and frequently selected  
31 method for the preparation of nanostructured materials. To date, various templating agents have  
32 been introduced for template-assisted methods in the form of additives and/or surfactants such as  
33 polymethylmethacrylate (PMMA) [5], polystyrene (PS) latex [6], and n-propyl amine [7]. Notably,  
34 only non-renewable resources that are hazardous and toxic are used to produce the additive or  
35 surfactant templates in the industries.

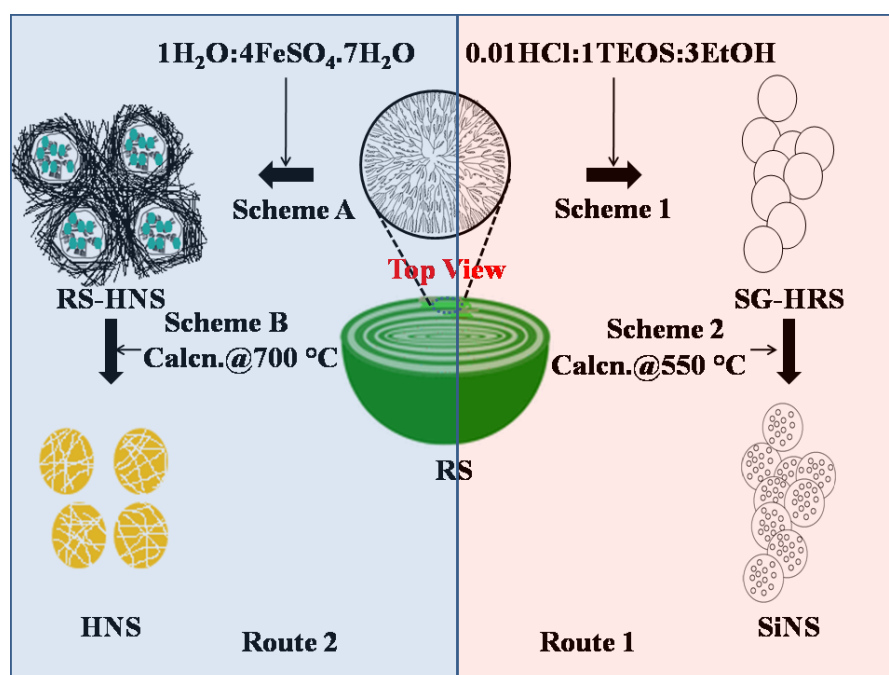
36 For environmentally-friendly approaches, starch has been successfully employed as green  
37 templates for the synthesis of nanostructured materials [8, 9]. In this way, the user of additives  
38 and/or surfactants template could be avoided and benign reagents from biomaterials can be  
39 introduced. In the case of starch, it is composed of linear amylose and branched amylopectin  
40 structures, that have hydroxyl (OH) and aldehyde (COH) as the functional groups. Previously, the  
41 OH and COH groups were recognized in facilitating adsorption of the desired precursors onto their  
42 reactive surfaces, for the synthesis of different nanostructured materials [9, 10]. Despite this interest,  
43 no one to the best of author's knowledge, utilized starch for the synthesis of different metals,

44 particularly metalloids and transition metals of silica and hematite. Herein, an environmentally  
 45 friendly and efficient route for the synthesis of nanostructured of both silica and hematite using rice  
 46 starch as a promising biomaterials template are presented.

## 47 2. Results and Discussion

48 The aim of this study was to prepare nanostructured metals of both silica (metalloids) and  
 49 hematite (transition metals). This is the first step towards enhancing the understanding for the  
 50 synthesis of the different type of metals. To illustrate, two synthesis methods represent by Route 1  
 51 and 2 that consisted of two synthetic preparations were designed, as shown in Figure 1. For Route 1,  
 52 the starting precursor of rice starch and hydrolyzed starch are denoted as rice starch (RS) and  
 53 hydrolysis of rice starch (HRS), respectively (Scheme 1). Subsequently, aqueous ethanol (EtOH) and  
 54 tetraethyl orthosilicate (TEOS) were added to the HRS for complete polycondensation of TEOS into a  
 55 sol-gel paste, which is referred to as SG-HRS before calcined to produce nanostructured silica (SiNS)  
 56 powder (Scheme 2).

57 As can be seen in Figure 1, the hematite was synthesized according to Route 2. In Scheme A, an  
 58 appropriate amount of  $\text{FeSO}_4 \cdot 7\text{H}_2\text{O}$ , HCl and RS were added to double distilled water heated to 70  
 59 °C. Then, the mixtures were left to room temperature before being filtered, washed with double  
 60 distilled water and dried in oven at 100 °C for overnight to produce a dark paste denoted as  
 61 RS-HNP, followed by calcination to 700 °C (heating rate of 5 °C/min), before slowly cooled to room  
 62 temperature (Scheme B). The collected reddish-brown powder of nanostructured hematite is  
 63 referred to as HNS.



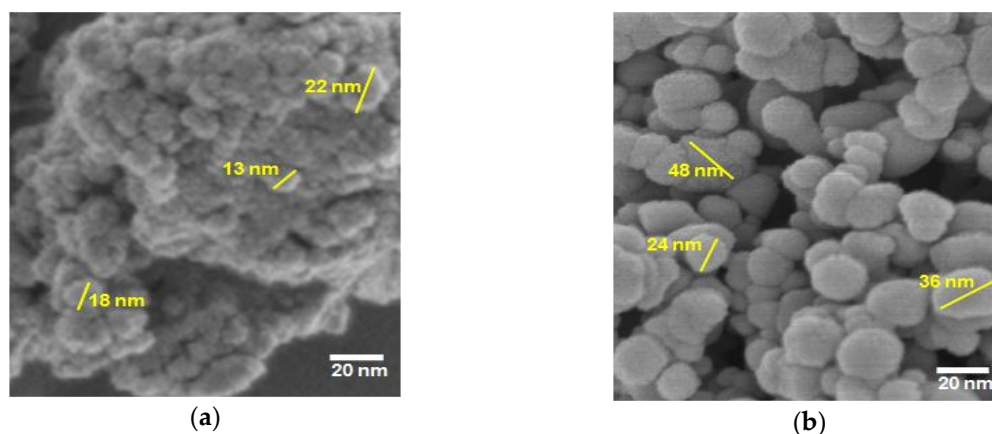
64

65 **Figure 1.** Preparation method for Route 1 of SiNS and Route 2 of HNS

### 66 2.1. Morphology Study

67 Figure 2 shows the FESEM micrograph for the synthesized metals of SiNS and HNS. In Figure  
 68 2(a), the FESEM micrograph image shows loose aggregation of pseudo-spherical morphology for  
 69 SiNS. Based on the FESEM image, SiNS were measured in the range of 13 to 22 nm diameters. It is  
 70 worth mentioning that partial macrophase separation during the sol-gel aging process and  
 71 subsequent sintering effect during calcination at high temperature had affected the SiNS uniformity.  
 72 In contrast, the HNS revealed almost monodispersed spherical-shaped nanoparticles as shown in  
 73 Figure 2(b). Judging from the FESEM image, HNS were spherical nanoparticles with sizes range of

74 24 to 48 nm. The steady growth of the hematite had uniformly nucleated which eventually form the  
 75 well ordered spherical structure of HNS. However, there is still a present of small agglomerations  
 76 that affect the HNS dispersity. From the FESEM images, it can thus be suggested that the SiNS from  
 77 SiO<sub>4</sub> frameworks is loosely nucleated, growth, and aggregated together in the presence of RS. The  
 78 weak interactions might be inherited from the nature of silica (Si) having metalloids characteristic  
 79 and thus, hindered the formation of ordered nanoparticles. In contrast, Fe precursor is strongly  
 80 bound together by metallophilic interactions [11] to give closely packed Fe<sub>2</sub>O<sub>3</sub> nanoparticles in the  
 81 RS, which promoted the formation of well ordered HNS.



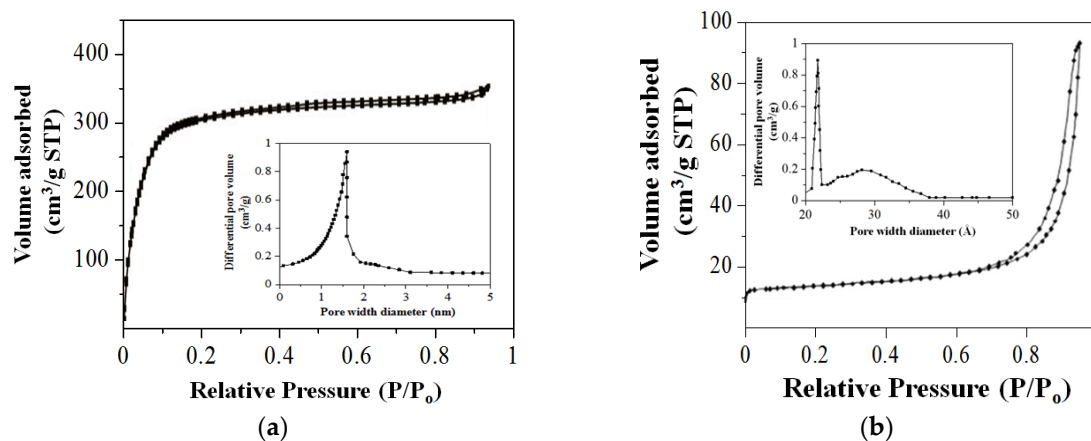
(a)

(b)

82 **Figure 2.** FESEM micrograph for: (a) SiNS; (b) HNS.

### 83 2.2. Physisorption Measurements

84 To quantify the surface area, the nitrogen (N<sub>2</sub>) physisorption measurements for SiNS and HNS  
 85 are presented in Figure 3. According to the IUPAC classification, the isotherms in Figure 3(a) for  
 86 SiNS are of a typical type I, which is significant for highly microporous materials. The primary  
 87 adsorption occurred at the low relative pressure of  $P/P_0 < 0.1$ , with the absence of a more rounded  
 88 'knee' indicating that the pore sizes were narrowed. As can be seen in Figure 3(b), HNS exhibits a  
 89 typical type-IV isotherm with H3-type hysteresis loop at the high relative pressure of  $P/P_0 > 0.6$ ,  
 90 which is significant for the mesopores networks, while the H3-type hysteresis loop is attributed to  
 91 slit-shaped pores. Based on the measurements, the calculated Brunauer-Emmett-Teller (BET) surface  
 92 area for SiNS and HNS has been experimentally determined to be 538.74 and 20.04 m<sup>2</sup>/g. The results  
 93 are consistent with other works for producing SiNS and HNS from biomaterials templates [12].  
 94 Furthermore, the average pore diameters for SiNS and HNS is determined based on the BJH model  
 95 to be 1.6 and 2.2 nm, respectively as shown in the inset in Figure 3. The surface area characteristics  
 96 were summarized in Table 1.



(a)

(b)

97 **Figure 3.** Physisorption measurements for (a) SiNS and (b) HNS. Inset represent Barrett, Joyner and  
 98 Halenda method (BJH) models.

99

**Table 1.** Physisorption measurements data for SiNS and HNS.

Sample	Surface area (m <sup>2</sup> /g)	Pore diameter (nm)
SiNS	538.74	1.6
HNS	20.04	2.2

Based on the morphology and physisorption measurements, it is suggested that the present of RS act as a template that effectively facilitates the formation of SiNS and HNS for nanostructured silica and hematite, respectively. The presence of RS not only gives ordered morphology but also aided the formation of porosity in both SiNS and HNS.

### 3. Materials and Methods

All reagents used in the study were used as received from analytical grade reagents.

#### 3.1. Preparation of Nanostructured Silica (SiNS)

SiNS were synthesized according to a calculated sol-gel composition of TEOS:H<sub>2</sub>O:HCl:CH<sub>3</sub>CH<sub>2</sub>OH at 1:4:0.01:3. Firstly, TEOS was added to an alcoholic acidified solution in the presence of HRS (38 wt %) at 60 °C for 6 h to produce SG-HRS. The SG-HRS was then calcined at 550 °C to give opal-white colored of SiNS.

#### 3.2. Preparation of Nanostructured Hematite (HNS)

HNS was synthesized according to a calculated composition of H<sub>2</sub>O:HCl:RS:FeSO<sub>4</sub>·7H<sub>2</sub>O at 1:0.002:1:4. Firstly, an appropriate amount of FeSO<sub>4</sub>·7H<sub>2</sub>O, HCl and RS were added to double distilled water, heated to 70 °C and constantly stirred for 1 h. Then, the mixtures were left to room temperature before being filtered, washed with double distilled water and dried in an oven at 100 °C for overnight to produce a dark paste of RS-HNS. Subsequently, the RS-HNS was heated to 700 °C (heating rate of 5 °C/min) and maintained, before slowly cooled to room temperature. Finally, the powder was treated with concentrated HCl, before the samples were finally dried and collected as reddish-brown powder which is referred to as HNS.

#### 3.3. Characterization

The morphology of particles was observed using field emission scanning electron microscopy (FESEM, JSM-6700F, JEOL, Tokyo, Japan). The nitrogen adsorption-desorption measurement is performed using AUTOSORB-1 Quantachrome volumetric adsorption analyzer by using nitrogen as the adsorbate at 77.35 K for full-scale adsorption-desorption isotherms (Boynton Beach, Florida, USA). The samples were degassed at 363 K for 3 h and held at 433 K for 12 h before analysis. A Barrett–Emmett–Teller (BET) model was used to calculate the specific surface area and a Barrett–Joyner–Halenda (BJH) model was used to calculate the pore volume distribution and the average pore size.

### 4. Conclusions

In summary, the nanostructured silica and hematite were successfully prepared using rice starch by a template-assisted synthesis. The SiNS showed a pseudo-spherical morphology with nano-sized from 13 to 22 nm, and surface area of 538.74 m<sup>2</sup>/g. On the other hand, the HNS showed a spherical-shaped morphology with nano-sized from 24 to 48 nm, and surface area of 20.04 m<sup>2</sup>/g. In the future, both synthesized SiNS and HNS could be used as a potential nano-catalysts owing to the ordered morphology and porous networks that facilitate optimum charge transfers process.

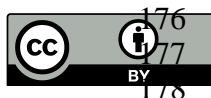
136

137 **Acknowledgments:** This work was financially supported by Universiti Teknologi Mara (UiTM, Malaysia)  
138 under research grants cost centre No. 600-IRMI-Dana KCM 5/3/LESTARI (118/2017) and No. 600-UiTMSEL (PI.  
139 5/4) (044/2018).

140 **Conflicts of Interest:** The author declare no conflict of interest.

## 141 References

- 142 1. Zhu, H.; Jing, Y.; Pal, M.; Liu, Y.; Liu, Y.; Wang, J.; Zhang, F.; Zhao, D. Mesoporous TiO<sub>2</sub>@ N-doped Carbon  
143 Composite Nanospheres Synthesized by the Direct Carbonization of surfactants After Sol-gel Process for  
144 Superior Lithium Storage. *Nanoscale*, **2017**, *9*, 1539-1546. DOI: 10.1039/C6NR08885F.
- 145 2. Ghiyasiyan-Arani, M.; Salavati-Niasari, M.; Masjedi-Arani, M.; Mazloom, F., An Easy Sonochemical Route  
146 for Synthesis, Characterization And Photocatalytic Performance of Nanosized FeVO<sub>4</sub> in The Presence of  
147 Aminoacids as Green Capping Agents. *J Mater Sci-Mater El*, **2018**, *29*, 474-485. DOI:  
148 10.1007/s10854-017-7936-9.
- 149 3. Zheng, Y.; Huang, Y.; Abbas, Z.M.; Benicewicz, B.C. One-Pot Synthesis of Inorganic Nanoparticle Vesicles  
150 Via Surface-Initiated Polymerization-Induced Self-Assembly. *Polym Chem*, **2017**, *8*, 370-374. DOI:  
151 10.1039/C6PY01956K.
- 152 4. Kothary, P.; Dou, X.; Fang, Y.; Gu, Z.; Leo, S.Y.; Jiang, P.; Superhydrophobic Hierarchical Arrays  
153 Fabricated By a Scalable Colloidal Lithography Approach. *J Colloid Interf Sci*, **2017**, *487*, 484-492. DOI:  
154 10.1016/j.jcis.2016.10.081.
- 155 5. Hyodo, T.; Fujii, E.; Ishida, K.; Ueda, T.; Shimizu, Y., Microstructural Control of Porous In<sub>2</sub>O<sub>3</sub> Powders  
156 Prepared by Ultrasonic-Spray Pyrolysis Employing Self-Synthesized Polymethylmethacrylate  
157 Microspheres as a Template and Their NO<sub>2</sub>-Sensing Properties. *Sensor Actuat B-Chem*, **2017**, *244*,  
158 992-1003. DOI: 10.1016/j.snb.2017.01.091.
- 159 6. Syoufian, A.; Inoue, Y.; Yada, M.; Nakashima, K., Preparation of Submicrometer-Sized Titania Hollow  
160 Spheres by Templating Sulfonated Polystyrene Latex Particles. *Mat Let*, **2007**, *61*, 1572-1575.  
161 DOI:10.1016/j.matlet.2006.07.081.
- 162 7. Hao, N.; Jayawardana, K.W.; Chen, X.; Yan, M., One-Step Synthesis of Amine-Functionalized Hollow  
163 Mesoporous Silica Nanoparticles as Efficient Antibacterial and Anticancer Materials. *ACS Appl Mater*  
164 *Inter*, **2015**, *7*, 1040-1045. DOI: 10.1021/am508219g.
- 165 8. Zan, G.; Wu, Q., Biomimetic and Bioinspired Synthesis of Nanomaterials/Nanostructures. *Adv Mat*, **2016**,  
166 *28*, 2099-2147. DOI: 10.1002/adma.201503215.
- 167 9. Matmin, J.; Affendi, I.; Endud, S., Direct-Continuous Preparation of Nanostructured Titania-Silica Using  
168 Surfactant-Free Non-Scaffold Rice Starch Template. *Nanomaterials*, **2018**, *8*. DOI: 10.3390/nano8070514.
- 169 10. Zhang, B.; Davis, S.A.; Mann, S., Starch Gel Templating of Spongelike Macroporous Silicalite Monoliths  
170 and Mesoporous Films. *Chem Mat*, **2002**, *14*, 1369-1375. DOI: 10.1021/cm011251p.
- 171 11. Otero-de-la-Roza, A.; Mallory, J.D.; Johnson, E.R.; Metallophilic Interactions from Dispersion-Corrected  
172 Density-Functional Theory. *J Chem Phys*, **2014**, *140*, 18A504. DOI: 10.1063/1.4862896.
- 173 12. Wu, C.; Wang, J.; Hu, Y.; Zhi, Z.; Jiang, T.; Zhang, J.; Wang, S. Development of a Novel Starch-Derived  
174 Porous Silica Monolith for Enhancing the Dissolution Rate of Poorly Water Soluble Drug. *Mater. Sci. Eng.*  
175 *C*, **2012**, *32*, 201-206. DOI: 10.1016/j.msec.2011.10.019.



© 2018 by the authors. Submitted for possible open access publication under the terms and conditions of the Creative Commons Attribution (CC BY) license (<http://creativecommons.org/licenses/by/4.0/>).